Int. J. Electrochem. Sci., 7 **(2012)** 1532 - 1542

International Journal of
ELECTROCHEMICAL
SCIENCE
www.electrochemsci.org

Investigation of Composite Nafion/Sulfated Zirconia Membrane for Solid Polymer Electrolyte Electrolyzer Applications

S. Siracusano[1,*], *V. Baglio*[1], *M.A. Navarra*[2], *S. Panero*[2], *V. Antonucci*[1], *A. S. Aricò*[1]

[1] CNR-ITAE, Via Salita S. Lucia sopra Contesse 5-98126 Messina, Italy
[2] Department of Chemistry, University of Rome "La Sapienza", P.le Aldo Moro 5-00185 Roma, Italy
[*]E-mail: siracusano@itae.cnr.it

Received: 13 December 2011 / *Accepted:* 28 December 2011 / *Published:* 1 February 2012

A composite Nafion-Sulfated Zirconia ($SZrO_2$) membrane was prepared and investigated in a solid polymer electrolyte (SPE) water electrolyzer at different temperatures. The performance was compared to a commercial Nafion 115 membrane of similar thickness. The cell equipped with Nafion – $SZrO_2$ showed better performance at intermediate temperatures. The current densities were 2.7 and 2.2 $A \cdot cm^{-2}$ at a terminal voltage of 1.8 V for the composite Nafion – $SZrO_2$ and Nafion 115, respectively, at 100°C and atmospheric pressure. The superior performance of the composite electrolyte was due to the strong acidity and water affinity of sulfated zirconia nanoparticles used as filler. Operation at intermediate temperatures in a solid polymer electrolyte water electrolyzer appears useful for a better thermal management of the heat released at high current densities.

Keywords: SPE electrolyzer; composite membrane; water electrolysis; solid polymer electrolyte.

1. INTRODUCTION

Solid polymer electrolyte (SPE) water electrolysis technology is considered a very interesting alternative to the more conventional alkaline water electrolysis. The advantages of SPE technology over the alkaline one are clearly established: high gas purity (more than 99.998% for hydrogen), possibility of producing compressed gases (up to 200 bars and more), increased level of safety (no circulating of caustic electrolyte), much smaller mass and overall dimensions, significantly lower power consumption [1-9].

The SPE electrolyzer utilizes as the anodic catalyst noble metal oxides, as Ru and Ir, due to their high electronic conductivity, chemical and thermal stability [10-28]. For the hydrogen evolution reaction, platinum provides the best performance and is commonly used as cathode catalyst. A proton exchange membrane (a perfluorosulfonic acid solid electrolyte membrane, such as Nafion® membrane)

as the electrolyte permits the transfer of protons from anode to cathode. Water splitting is an endothermic process. If no external heat is supplied, it can occur at a cell voltage larger than the thermoneutral potential (E_{tn}) of 1.48 V [7] according to the following thermodynamic equation:

$$E_{tn} = \Delta H/nF$$

However, to reduce capital costs, polymer electrolyte membrane water electrolyzers (PEMWEs) are operated at around 2 V/cell allowing the achievement of high current densities (better than 1 $A \cdot cm^{-2}$). The corresponding heat released in each cell due to the irreversibility of the process is typically larger than 0.5 W_{th}/cm^2. In a polymer electrolyte membrane water electrolyzer stack of 1 Nm^3/h capacity, the heat released under such operating conditions thus exceeds 1 kW_{th}. The conventional operating temperature of a PEMWE is around 80 °C; however high speed water recirculation is necessary to maintain this temperature and an additional cooling set up using large radiator and/or external blower is necessary.

A wider range of operating temperature e.g. up to 100 °C may result in a better water and thermal management especially under the low pressure regime. High pressure operation will help to maintain a good fraction of liquid water inside the polymer electrolyte membrane, however standard Nafion membranes suffer from a decreased proton conductivity at above 100 °C even under such conditions [29]

Modification of Nafion with formation of composite Nafion-based membranes has been object of different studies [29-41]. These composite structures should allow an increase of the operating temperature enhancing in this way the oxygen evolution reaction rate, which is the rate determining step of this process. Also the use of phosphoric acid doped polybenzimidazole (PBI) membranes was investigated to increase the operating temperature of an SPE electrolyzer [42]. These approaches allowed to obtain high current density with good conversion efficiency [29,30,42].

On the other hand, the sulfated metal oxides have become subjects of intensive studies, being more stable than other solid superacids [31, 43]. In general, the incorporation of inorganic solid acids in conventional Nafion-type membranes is of interest, having the dual function of improving water retention as well as providing additional acidic sites [44]. Currently, sulfated zirconia ($SZrO_2$) is recognized as one of the strongest superacid among all known solids ($H_o < -16$) [45]. It has been demonstrated that the proton conductivity of sulfated zirconia, as well as its surface and crystallographic properties, varies largely depending on the method of preparation, in particular on the thermal treatments [46,47]. Introducing $SZrO_2$ in Nafion membranes, a general enhancement was revealed in the fuel cell response, both in terms of power density delivered and reduction of ohmic resistance, compared to unmodified Nafion membranes. Moreover, the high-temperature impedance response of the $SZrO_2$-doped Nafion-based fuel cell was highly improved, showing a well-controlled charge-transfer resistance [48].

Despite the composite $SZrO_2$-doped membrane appears promising in fuel cells, no previous attempts were made to investigate its behaviour in a PEM water electrolyzer.

The objective of this work is to study the application of a composite Nafion - $SZrO_2$ membrane as the electrolyte in an PEM water electrolyzer in order to increase the operating temperature,

improving, thus, the performance and allowing better thermal and water management under practical applications.

2. EXPERIMENTAL

2.1 Membrane electrodes assembling (MEA)

Both sulphated zirconia, having a tetragonal crystalline structure, and $SZrO_2$/Nafion composite membranes were prepared according to procedures previously reported [31]. A Nafion 115 (Ion Power) membrane was used for comparison. The thickness of the composite membranes was about 120 μm in the dry form, comparable to Nafion 115. A sulfite-complex route, described in detail in Ref. [11], was used to prepare the anodic IrO_2 electrocatalyst. A slurry composed of 67 wt.% catalyst and 33 wt.% Nafion ionomer (5 wt.% Ion Power solution) in deionised water and anhydrous Ethylic alcohol (Carlo Erba) was prepared by mixing under ultrasounds. This slurry was directly deposited onto one face of the membrane by using a spray technique. The anode catalyst loading was 2.5 $mg \cdot cm^{-2}$. A Ti grid (Franco Corradi, Italy) was used as the backing layer for the anode. A commercial 30% Pt/Vulcan XC-72 (ETEK, PEMEAS, Boston, USA) was used as the catalyst for the H_2 evolution. The cathode catalyst was spread on carbon cloth backings (GDL ELAT from ETEK) with a Pt loading of 0.5 $mg \cdot cm^{-2}$. The ionomer content in both electrodes was 33 wt.% in the catalytic layer after drying. MEAs (5 cm^2 geometrical area) were directly prepared in the cell housing by tightening at 9 N·m using a dynamometric wrench.

2.2 MEA electrochemical characterization

The 5 cm^2 PEM single cell electrolyzer performance was evaluated at different temperatures (80° and 100°C) and under atmospheric pressure. Deionised water was pre-heated at the same cell temperature and supplied by a pump at a flow rate of 2 $ml \cdot min^{-1}$ to the anode compartment. The water temperature was maintained at the same temperature of the cell by proper heat supply. Measurements of cell potential as a function of current density, electrochemical impedance spectroscopy (EIS) and chrono-amperometry were carried out by an Autolab PGSTAT 302 Potentiostat/Galvanostat equipped with a 20 A booster (Metrohm). The impedance measurements were performed under potentiostatic control in a frequency range between 20 kHz and 0.1 Hz by frequency sweeping in the single sine mode.

The amplitude of the sinusoidal excitation signal was 0.01 V. The series resistance was determined from the high frequency intercept on the real axis of the Nyquist plot. The polarization resistance was taken as the difference between the extrapolated low frequency intercept and the high frequency intercept on the real axis.

The morphology of the composite Nafion/sulfated zirconia membrane was investigated by using scanning electron microscopy SEM-FEG (FEI XL 30)–instrument.

3. RESULTS AND DISCUSSION

The polarization curves for the electrolysis cells based on bare Nafion and composite membrane at 80°C and under atmospheric pressure are reported in Figure 1.

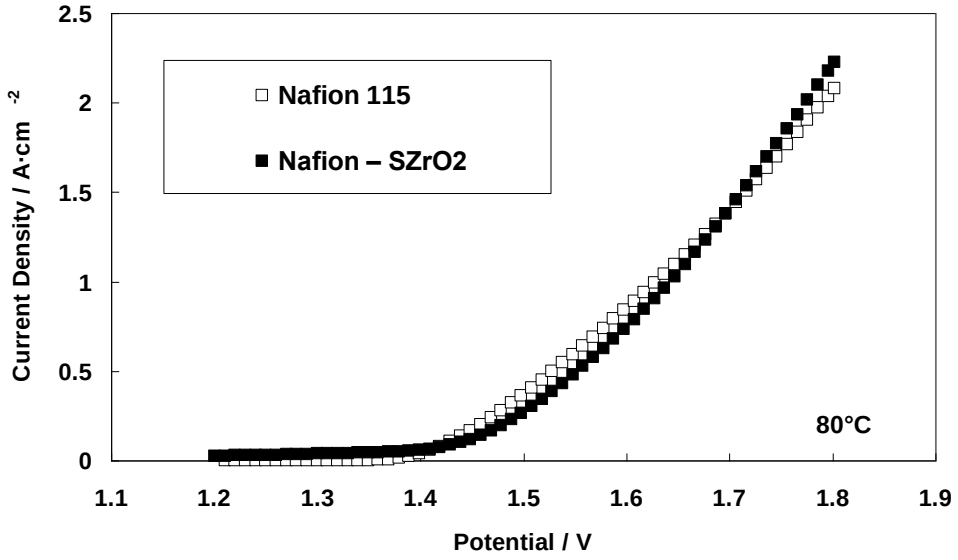

Figure 1. Polarization curves for the electrolyzers with different membranes at 80 °C

A slight different trend for the two electrolysis cells is observed. The performance in the activation (current onset) region is better for the cell with Nafion 115, indicating a better catalyst-electrolyte interface; whereas at high potential values, where electrolyte conductivity is predominant, the cell with Nafion – $SZrO_2$ shows a better behaviour.

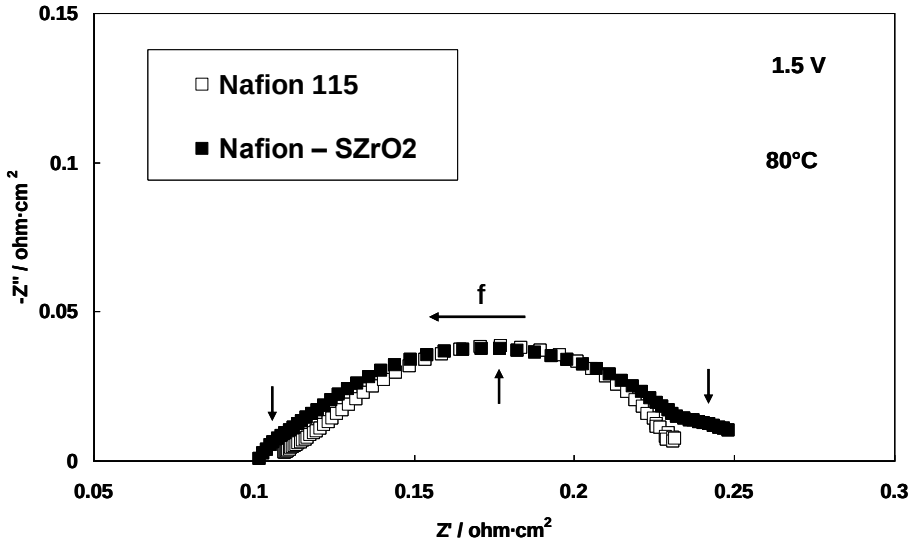

Figure 2. Nyquist plots for the electrolyzers with different membranes at 80 °C

To get more insights on the different characteristics of the two MEAs, an analysis of the electrochemical impedance was carried out at 1.5 V and 80 °C on the two cells. A comparison of Nyquist plots is reported in Figure 2. The series resistance of the cell equipped with the composite membrane is slightly lower. This value is around 0.1 $\Omega \cdot cm^2$. Thus under a high humidification level (liquid water is fed to the cell at 80°C), the conductivity of the composite membranes is just slightly better than bare Nafion producing a more favourable slope in the polarization curve at high current density where ohmic drop is predominant. Instead, the polarization resistance at 1.5 V is slightly lower for the cell with Nafion 115 (0.13 $\Omega \cdot cm^2$ vs. 0.15 $\Omega \cdot cm^2$), as a result of a better interface between catalysts and bare membrane. This difference is confirmed also by the polarization curve (Fig. 1) where a higher current is observed at 1.5 V for bare Nafion 115. The composite membrane shows an additional semicircle at low frequencies which may be related to mass transport constraints e.g. a slow removal of the reaction products at the catalyst-electrolyte interface.

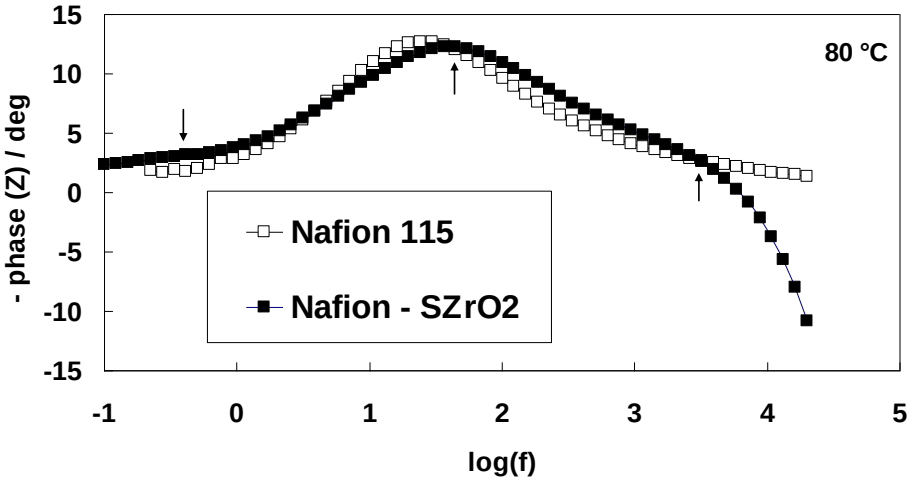

Figure 3. Bode plots for the electrolyzers with different membranes at 80 °C

Comparison of the phase response as a function of frequency in the Bode plots for the impedance spectra (Fig. 3) allows to identify three relaxation times at high (2615 Hz), intermediate (44.7 Hz) and low (0.41 Hz) frequencies for the composite membrane. The relaxation process at high frequency is possibly associated to the H_2 evolution. This corresponds to a very small semicircle (at around 0.1 $\Omega \cdot cm^2$ for the composite membrane) in the Nyquist plot of Fig. 2. Whereas the one at intermediate frequency, corresponding to the main semicircle in Fig. 2, is related to the oxygen evolution that is the limiting step of the entire process. The occurrence of a relaxation process at very low frequencies for the composite membrane (Fig. 3), related to the small semicircle at around 0.24 $\Omega \cdot cm^2$ in Fig. 2, is indicative of transport related characteristics. Non optimal membrane-catalyst combination may probably affect the speed of gas removal at the interface.

In figure 4 chrono-amperometric measurements for the two different electrolysis cells, at 1.6 V and 80 °C, are reported. The electrolyzer containing Nafion – $SZrO_2$ as the membrane, though has lower performance compared to the electrolyzer with Nafion 115, has shown lower decay during the

time stability test with a stable value of 0.72 $A \cdot cm^{-2}$ @ 1.6 V. Generally, the presence of an inorganic filler inside the membrane reduces cross over effects improving the stability with time.

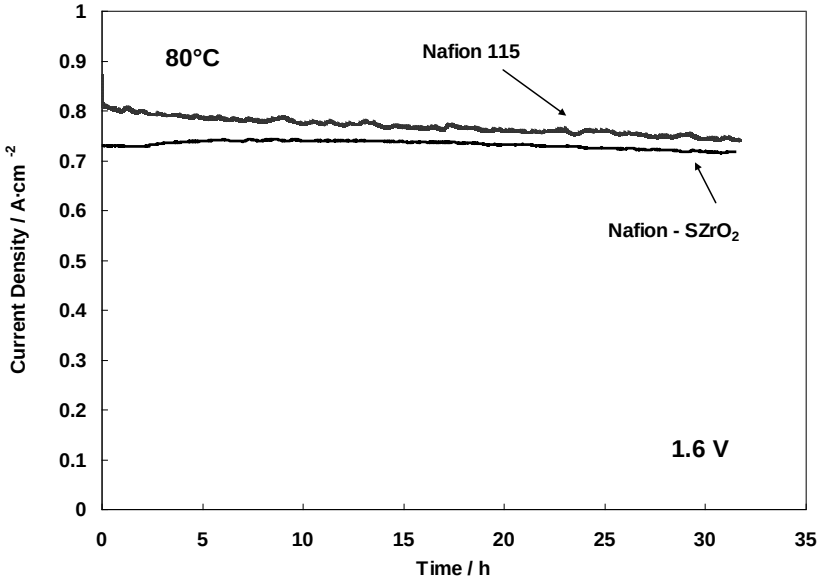

Figure 4. Chrono-amperometric measurements at 1.6 V and 80°C for the electrolyzers with different membranes

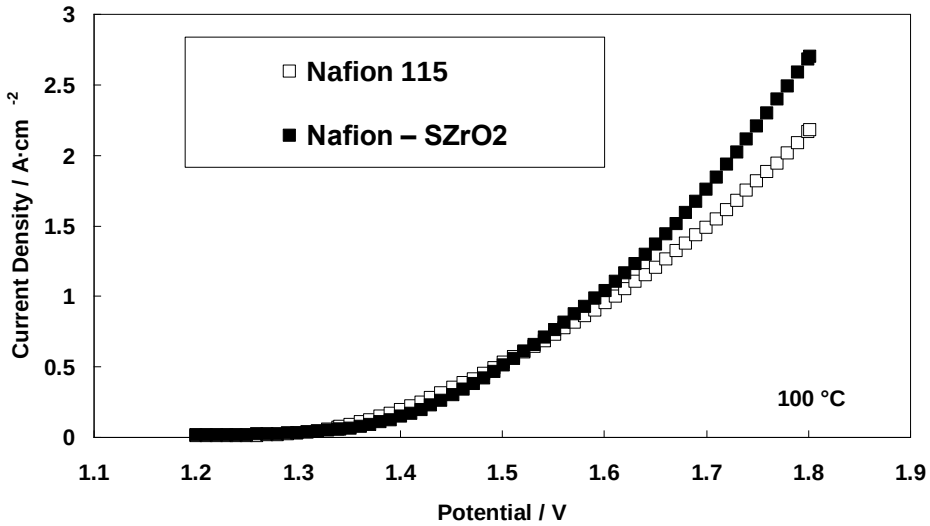

Figure 5. Polarization curves for the electrolyzers with different membranes at 100 °C

In order to evaluate the properties of the Nafion – $SZrO_2$ membrane at higher temperatures, the polarization curves of the two electrolyzers were performed at 100 °C and atmospheric pressure (Figure 5). Better overall performances are achieved at high temperatures and full humidification. The polarization curve for the cell based on Nafion – $SZrO_2$ showed higher performance compared to the

cell with Nafion 115. Especially in the practical range of current densities, the differences are more significant above 1.55 V. At 1.8 V, the current density for water splitting was 2.7 $A \cdot cm^{-2}$ for the composite membrane and 2.2 $A \cdot cm^{-2}$ for the bare Nafion membrane corresponding to an increase of about 20 %.

This is due to the good conductivity of the membrane compared to the Nafion 115 at this temperature (100 °C). Previous studies related to the application of this composite membrane in fuel cell revealed improved proton diffusivity as indicated by NMR studies [31].

The perspectives of sulfated zirconia on Nafion properties for PEM electrolyzer application are demonstrated. The superacidic inorganic compound appears to promote higher hydration level in the composite membranes with respect to a bare Nafion membrane, as demonstrated in a previous paper dealing with fuel cells [31] and using water uptake measurements. The presence of the inorganic compound resulted also in higher water diffusion coefficients for the doped membranes over a wide range of temperature and external relative humidity (i.e., 30-100%) [31]. Impedance spectroscopy measurements provided an in situ confirmation of these enhanced properties.

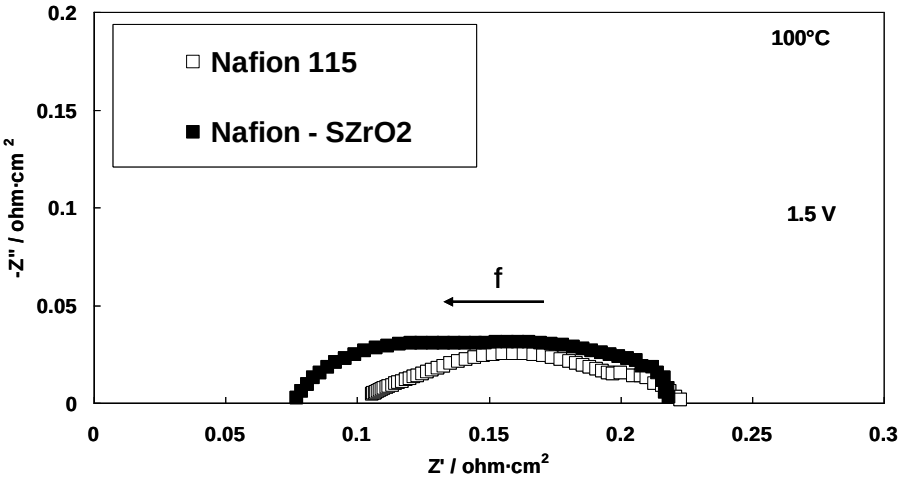

Figure 6. Nyquist plots for the electrolyzers with different membranes at 100 °C and 1.5 V

A comparison of the Nyquist plots for the two electrolysis cells at high temperature (100 °C) in the activation controlled region (1.5 V) is reported in Figure 6. As reported above, similar series resistance was observed for the two membranes at 80 °C (see Fig. 3), whereas significantly lower series resistance (Fig. 6) was obtained at high temperatures (100 °C) for the cell equipped with the composite membrane with respect to that containing bare Nafion (0.075 $\Omega \cdot cm^2$ vs. 0.1 $\Omega \cdot cm^2$). This confirms the improved proton and water diffusivity of the Nafion – $SZrO_2$ membrane compared to the bare membrane at higher temperatures.

The Nyquist plot profiles are significantly different at 100 °C than at 80 °C especially for the composite membrane showing the presence of two semicircles contributing in a similar extent to the overall impedance; whereas, at 80 °C the high frequency semicircle related to the electrochemical oxygen evolution process was dominant. The high temperature operation considerably reduces the

activation barrier for oxygen evolution. However, it appears evident an increase of mass transport constraints (low frequencies semicircle) probably related to the removal of reaction products which may be slightly hindered by a more consistent vapour phase at the interface at 100 °C. The linear slope at high frequencies at 100 °C in the Nafion 115 membrane appears related to some hydration constraints. Hydrogen evolution on Pt should not give a relevant contribution to the impedance spectra at 100 °C. Its very low relaxation time is indicative of the occurrence of a very small semicircle at high frequency that is not evident at 100 °C but it is envisaged for the composite membrane at 80 °C. The Bode plots show essentially two main relaxation times for the composite membrane and Nafion at 100 °C (Fig. 7).

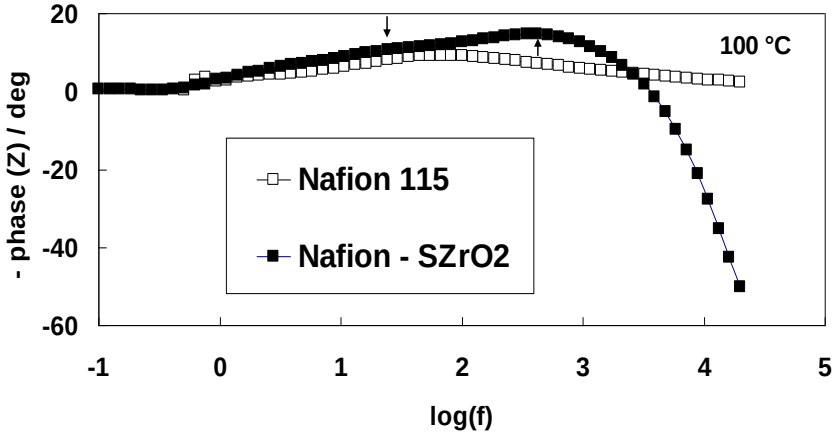

Figure 7. Bode plots for the electrolyzers with different membranes at 100 °C

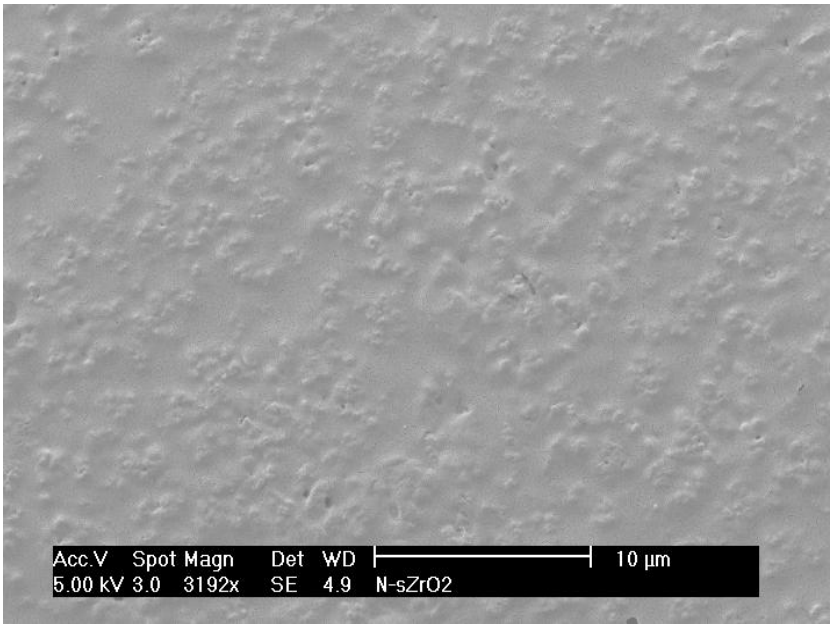

Figure 8. SEM image of composite Nafion – $SZrO_2$ membrane

As shown by the impedance spectra at 100 °C, the catalyst-electrolyte interface is not yet optimised for the composite membrane as shown by the occurrence of larger polarization resistance. The latter is exacerbated by the presence of a consistent low frequency semi-circle.

To better understand the origin of the increased polarization resistance for the composite membrane with respect to Nafion, we have investigated the surface morphology of the composite polymer inorganic material (Fig. 8) by scanning electron microscopy (SEM). It appears at low magnification that the filler is evenly distributed; but, on a microscopic scale, the occurrence of agglomerates of inorganic filler extending about 500 nm in diameter and bare perfluorosulfonic acid regions is quite clear. The agglomerates form surface protuberances which may reduce the adhesion of the catalytic layer on the composite membrane. The adhesion is instead optimal for the microscopically flat bare Nafion membrane.

4. CONCLUSIONS

The properties of a composite Nafion – $SZrO_2$ membrane for SPE electrolyzers were compared to those of a commercial membrane, Nafion 115. The composite membrane showed promising properties for both conventional (80 °C) and high temperature operation allowing the achievement of higher performance at 100 °C under practical operating conditions corresponding to suitable current density. A higher working temperature allowed the increase in the electrolyzer performance thanks to the enhanced reaction kinetics, in particular at the anode of the electrolyzer. The enhancement of performance of the composite membrane versus bare Nafion appears essentially related to an increase of conductivity; whereas it still remains unoptimized the catalyst-electrolyte interface under the new configuration. The gain in performance due to the increased proton conductivity in the composite membrane is counteracted in part by the increase of polarization resistance. These aspects need to be addressed in a next study in order to allow for a more significant increase in performance with the new polymer electrolyte.

ACKNOWLEDGMENT
Authors from CNR-ITAE acknowledge the financial support from "Ministero dello Sviluppo Economico - Accordo di Programma MSE-CNR per la Ricerca di Sistema elettrico Nazionale". M.A. Navarra acknowledge the financial support of Sapienza University of Rome, Progetto Ateneo 2010 "Synthesis and physical chemical characterizations of proton conducting, nano-composite polymer electrolytes for fuel cell application".

References

1. S.A. Grigoriev, V.I. Porembsky, V.N. Fateev, *Int J Hydrogen Energy*, 31 (2006) 171.
2. E. Slavcheva, I. Radev, S. Bliznakov, G. Topalov, P. Andreev, E. Budevski, *Electrochim Acta*, 52 (2007) 3889.
3. B. Borresen, G. Hagen, R. Tunold, *Electrochim. Acta*, 47 (2002) 1819.
4. F. Marangio, M. Santarelli, M. Calì, *Int J Hydrogen Energy*, 34 (2009) 1143.

5. M. Santarelli, P. Medina, M. Calì, *Int J Hydrogen Energy*, 34 (2009) 2519.
6. P. Millet, D. Dragoe, S. Grigoriev, V. Fateev, C. Etievant, *Int J Hydrogen Energy*, 34 (2009) 4974.
7. P. Millet, R. Ngameni, S.A. Grigoriev, N. Mbemba, F. Brisset, A. Ranjbari, C. Etiévant, *Int J Hydrogen Energy*, 35 (2010) 5043.
8. L. Ma, S. Sui, Y. Zhai, *Int J Hydrogen Energy*, 34 (2009) 678.
9. S.A. Grigoriev, P. Millet, S.V. Korobtsev, V.I. Porembskiy, M. Pepic, C. Etievant, C. Puyenchet, V.N. Fateev, *Int J Hydrogen Energy*, 34 (2009) 5986.
10. J.C. Cruz, V. Baglio, S. Siracusano, V. Antonucci, A.S. Aricò, R. Ornelas, L. Ortiz-Frade. S, M. Durón-Torres, L.G. Arriaga. Preparation and Characterization of RuO_2 Catalysts for Oxygen Evolution in a Solid Polymer Electrolyte. *Int. J. Electrochem. Sci*., 6 (2011) 6607.
11. S. Siracusano, V. Baglio, A. Stassi, R. Ornelas, V. Antonucci, A.S. Aricò, *Int J Hydrogen Energy*, 36 (2011) 7822.
12. J.C. Cruz, V. Baglio, S. Siracusano, R. Ornelas, L. Ortiz-Frade, L.G. Arriaga, V. Antonucci, A.S. Aricò, *Journal of Nanoparticle Research*, 13 (2011) 1639.
13. S. Siracusano, V. Baglio, A. Di Blasi, N. Briguglio, A. Stassi, R. Ornelas, E. Trifoni, V. Antonucci, A.S. Aricò, *Int J Hydrogen Energy*, 35 (2010) 5558.
14. S. Siracusano , A. Di Blasi, V. Baglio, G. Brunaccini, N. Briguglio, A. Stassi, R. Ornelas, E. Trifoni, V. Antonucci, A.S. Aricò, *Int J Hydrogen Energy*, 36 (2011) 3333.
15. S. Siracusano, V. Baglio, N. Briguglio, G. Brunaccini, A. Di Blasi, A. Stassi, R. Ornelas, E. Trifoni, V. Antonucci, A.S. Aricò. An electrochemical study of a PEM stack for water electrolysis *Int J Hydrogen Energy* (2011), doi:10.1016/j.ijhydene.2011.06.019.
16. A.Marshall, B. Børresen, G. Hagenm, M. Tsypkin, R. Tunold, *Mater Chem Phys*, 94 (2–3) (2005) 94226.
17. A.Marshall, M. Tsypkin, B. Børresen, G.K. Hagen, R. Tunold, *J. New Materials Electrochem Syst.*, 7 (2004) 197.
18. S. Trasatti, *Electrochim. Acta*, 29 (11) (1983) 1503.
19. S. Trasatti, *Electrochim. Acta*, 36 (2) (1991) 225.
20. F. Andolfatto, R. Durand, A. Michas, P. Millet, P. Stevens, *Int. J. Hydrogen Energy*, 19 (1994) 421.
21. P. Millet, F. Andolfatto, R. Durand, *Int. J. Hydrogen Energy*, 21 (1996) 87.
22. M. Yamaguchi, K. Ohisawa, T. Nakanori, Proceedings of the Intersociety Energy Conversion Engineering Conference, 3-4 (1997) 1958.
23. K. Ledjeff, F. Mahlendorf, V. Peinecke, A. Heinzel, *Electrochim. Acta*, 40 (3) (1995) 315.
24. E. Rasten, G. Hagen, R. Tunold, *Electrochim. Acta*, 48 (25-26) (2003) 3945.
25. J.M. Hu, J.Q. Zhang, C.N. Cao, *Int. J. of Hydrogen Energy*, 29 (2004) 791.
26. S. Song, H. Zhang, X. Ma, Z. Shao, R.T. Baker, B. Yi, *Int J Hydrogen Energy*, 33 (2008) 4955.
27. L. Nanni, S. Polizzi, A. Benedetti, A. De Battisti, *J. Electrochem Soc*., 146(1) (1999) 220.
28. A.De Oliveira-Sousa, M.A.S. da Silva, L.A. Avaca, P. Lima-Neto, *Electrochim. Acta*, 45 (27) (2000) 4467.
29. V. Antonucci, A. Di Blasi, V. Baglio, R. Ornelas, F. Matteucci, J. Ledesma-Garcia, L.G. Arriaga, A.S. Arico`, *Electrochim Acta*, 53 (2008) 7350.
30. V. Baglio, R. Ornelas, F. Matteucci, F. Martina, G. Ciccarella, I. Zama, L.G. Arriaga, V. Antonucci, A.S. Aricò, *Fuel Cells* 09, (3) (2009) 247.
31. A.D'Epifanio, M. A. Navarra, F. C. Weise, B. Mecheri, J. Farrington, S. Licoccia, S. Greenbaum, *Chem. Mater*., 22 (2010) 813.
32. Q. Li, C. Xiao, H. Zhanga, F. Chen, P. Fang, M. Pana, *J. Power Sources* 196 (2011) 8250.
33. G. Alberti, M. Casciola, *Annu. Rev. Mater. Res*., 33 (2003) 129.
34. V. Baglio, A. Di Blasi, A.S. Aricò, V. Antonucci, P.L. Antonucci, F. Nannetti, V. Tricoli, *Electrochimic. Acta*, 50 (2005) 5181.
35. K.A. Mauritz, J.T. Payne, *J. Membr. Sci*., 168 (2000) 39.

36. N.H. Jalani, K. Dunn, R. Datta, *Electrochim. Acta*, 51 (2005) 553.
37. K.T. Adjemian, R. Dominey, L. Krishnan, H. Ota, P. Majsztrik, T. Zhang, J. Mann, B. Kirby, L. Gatto, M. Velo-Simpson, J. Leahy, S. Srinivasan, J.B. Benziger, A.B. Bocarsly, *Chem. Mater*., 18 (2006) 2238.
38. A.S. Aricò, V. Baglio, A. Di Blasi, V. Antonucci, *Electrochem. Commun*., 5 (2003) 862.
39. H. Tang, Z. Wan, M. Pan, S. Jiang, *Electrochem. Commun*., 9 (2007) 2003.
40. K. Li, G. Ye, J. Pan, H. Zhang, M. Pan, *J. Membr. Sci*., 347 (2010) 26.
41. S. Chen, C. Han, C. Tsai, J. Huang, Y. Chen-Yang, *J. Power Sources*, 171 (2007)363.
42. D. Aili, M.K. Hansen, C. Pan, Q. Li, E. Christensen, J.O. Jensen, N.J. Bjerrum, *Int. J. Hydrogen Energy*, 36 (2011) 6985.
43. M.A. Navarra, C. Abbati, B. Scrosati, *J. Power Sources*, 183 (2008) 109.
44. T.M. Thampan, N.H. Jalani, P. Choi, R. Datta, *J. Electrochem. Soc.*, 152 (2005) A316.
45. G.D. Yadav, J. Nair, *J. Microporous Mesoporous Mater*., 33(1999) 1.
46. S. Hara, M. Miyayama, *Solid State Ionics*, 168 (2004) 111.
47. C. Li, M. Li, *J. Raman Spectrosc*., 33 (2002) 301.
48. M.A. Navarra, C. Abbati, F. Croce, B. Scrosati, *Fuel Cells*, 9 (2009) 222.